Appl. Phys. B 57, 243–248 (1993)

Applied Physics B Photophysics and Laser Chemistry

The Effects of Collisional Quenching on Degenerate Four-Wave Mixing

P. M. Danehy[1], **E. J. Friedman-Hill**[2], **R. P. Lucht**[2], **R. L. Farrow**[2]

[1] High Temperature Gasdynamics Laboratory, Stanford University, Stanford, CA 94305-3032, USA
(Tel.: +1-415/723-1823, Fax: +1-415/723-1748)
[2] Combustion Research Facility, Sandia National Laboratories, Livermore, CA 94551-0969, USA
(Tel.: +1-510/294-3259, Fax: +1-510/294-2276)

Received 10 May 1993/Accepted 6 August 1993

Abstract. We report a theoretical and experimental investigation of the effects of collisional quenching on resonant degenerate four-wave mixing (DFWM). Using single-mode laser radiation, peak signal intensity measurements were performed on an isolated line in the $A-X$ transition of NO. By using appropriate mixtures of N_2 and CO_2 as buffer gases, we varied the collisional quenching rate over several orders of magnitude while maintaining a fixed total collisional dephasing rate. The mixtures had approximately 100 Torr total pressure and were at room temperature. For I/I_{sat} approximately equal to 0.02, DFWM intensities were found to be less affected by variations in quench rate than were laser-induced fluorescence (LIF) intensities (I and I_{sat} are the pump laser and one-photon saturation intensities, respectively). Moreover, for I/I_{sat} roughly equal to 0.5, DFWM intensities were observed to be nearly independent of quench rate. The results are compared to two theoretical predictions, with good agreement observed. Both theories indicate that the minimum sensitivity of DFWM to quenching occurs near $I/I_{sat} \approx 1$.

PACS: 34.30.+h, 42.65.−k, 33.50.−j

Collisional quenching is a non-radiative process which competes directly with spontaneous emission, or fluorescence, during the relaxation of electronically excited molecules. In general, the efficiency of collisional quenching can depend on collision partner, pressure, temperature, and rotational quantum number. These dependencies can complicate the use of laser-induced fluorescence (LIF) to obtain quantitative measurements in reactive environments. Several methods attempting to account for the effects of quenching on LIF measurements have met with some success [1]. However, a technique that is inherently less dependent on quenching would be potentially more quantitative as it would depend less critically on knowledge of the collisional environment and the quench rates.

Degenerate four-wave mixing (DFWM) has recently been shown to hold considerable potential as a quantitative probe of gaseous media. Capabilities have been demonstrated for concentration mapping [2], temperature mapping [3] single-shot temperature measurement [4, 5], and concentration and temperature measurements in a plasma [6].

Evidence that DFWM intensities are relatively insensitive to collisional quenching has been reported by Dreier and Rakestraw [7]. They compared flame temperature measurements obtained from Boltzmann analyses of OH rotational DFWM intensities to coherent anti-Stokes Raman spectroscopy (CARS) of N_2. Excellent agreement between the two techniques was achieved without applying rotational-level (N) dependent quenching corrections to the DFWM intensities, even though such corrections are necessary to obtain accurate temperatures from unsaturated LIF measurements.

Here we report an investigation of the dependence of DFWM intensities on the collisional depopulation rates resulting from electronic quenching and rotational energy transfer (RET). DFWM intensity measurements were performed on trace quantities of NO in various mixtures of N_2 and CO_2, with compositions prepared to maintain a constant coherence dephasing rate (γ_{12}) and NO partial pressure. The CO_2 quench rate of the excited A state of NO is known to be roughly 10^4 times that of N_2 at room temperature [8]. To the extent that RET rates of NO are similar for collisions with N_2 and CO_2, relative intensity measurements in the different mixtures mainly probe the influence of the varying quench rate. We compare results obtained using nearly non-saturating and saturating laser intensities with a steady-state theory for stationary atoms [9] and with a time-dependent calculation obtained by numerically integrating the velocity-dependent density-matrix equations [10]. We also compare LIF and DFWM intensities measured under the same conditions.

1 Theory

Theoretical treatments of DFWM that include collisional effects have addressed collision-broadened stationary absorbers, and Doppler- and collision-broadened moving ab-

sorbers [9]. Stationary-absorber theory was derived for two-level saturable absorbers and arbitrarily high pump-laser intensities. For moving absorbers, exact analytic solutions for two-level systems have been obtained only for low laser intensity using perturbation theory. However, high-intensity effects in moving absorbers can be calculated by direct numerical integration (DNI) of the velocity-dependent density matrix equations, yielding results applicable over a wide range of laser intensities and relaxation rates. Both approaches include relaxation effects via the population and coherence decay rates, Γ_0 and γ_{12}, respectively.

According to the stationary-absorber theory, for very low laser intensities ($I/I_{sat} \ll 1$, where I is the pump intensity and I_{sat} is the one-photon saturation intensity) the line-center DFWM signal intensity I_{sig} depends on Γ_0 and γ_{12} as

$$I_{sig} \propto \Gamma_0^{-2}\gamma_{12}^{-4}, \tag{1}$$

where

$$\gamma_{12} = \tfrac{1}{2}(\gamma_1 + \gamma_2) + \gamma_{\text{Pure Dephasing}}, \tag{2}$$

$$\Gamma_0^{-1} = \tfrac{1}{2}(\gamma_1^{-1} + \gamma_2^{-1}). \tag{3}$$

γ_1 and γ_2 refer to population transfer rates for the lower and upper levels, respectively, and $\gamma_{\text{Pure Dephasing}}$ refers to the rate of elastic dephasing collisions [9, 11]. For the NO molecule we assume

$$\gamma_1 = \gamma_{\text{RET1}} + \gamma_{\text{VET1}}, \tag{4}$$

$$\gamma_2 = \gamma_{\text{RET2}} + \gamma_{\text{VET2}} + \gamma_{\text{Natural}} + \gamma_{\text{Quench}}. \tag{5}$$

Here, γ_{Natural} refers to the spontaneous emission rate, γ_{RET} refers to the rotational energy transfer rate, γ_{VET} is the vibrational energy transfer (VET) rate and γ_{Quench} is the quenching rate. The VET contributions are neglected in (4) and (5) because we excite only the lowest vibrational levels of NO, which have long vibrational lifetimes [12]. Furthermore, in this experiment γ_{Natural} is much smaller than γ_{RET} and γ_{Quench}, so that γ_{12} is dominated by collisional broadening. Thus, quenching enters into the DFWM signal equation as a contribution added to the RET rate rather than as a multiplicative factor. This quenching dependence contrasts with typical unsaturated LIF experiments where $I_{\text{LIF}} \propto 1/\gamma_{\text{Quench}}$ [1]. In writing (2), (4), and (5) in this form we have implicitly assumed statistical independence of the collisional processes.

2 Experiment

The experimental setup used a phase-conjugate geometry and was similar to that described in Reference 13. The laser source was a single-longitudinal-mode, pulse-amplified ring-dye laser, frequency-doubled and mixed with the Nd:YAG fundamental to obtain $\sim$ 1.0 mJ pulses tunable near 226 nm. The pulses had a bandwidth of 0.004 cm^{-1} and a duration of 10 ns. We typically used 12–300 μJ per pulse for each pump beam and one-fourth as much energy for the probe beam. All beams were collimated to a diameter of $\sim$ 2.5 mm and had vertical polarization. Measurements were performed on $\sim$ 30 mTorr of NO in approximately 100 Torr of N_2, CO_2, or a mixture of these two gases, contained in static cell with windows spaced 13 cm apart. This concentration of NO resulted in a line-center absorption of 6–7% in one pass. The operating pressure of 100 Torr was chosen to minimize thermal-grating contributions, and corresponds to a collision rate roughly one-half that of atmospheric-pressure flames.

DFWM and LIF signal intensities were simultaneously detected using photomultiplier tubes. Interference filters were placed in front of the DFWM detector ($\lambda_{\text{center}} =$ 220 nm, $\Delta\lambda_{\text{bandpass}} =$ 23 nm) and LIF detector ($\lambda_{\text{center}} =$ 250 nm, $\Delta\lambda_{\text{bandpass}} =$ 10 nm). In all measurements, we probed a well-isolated $O_{12}(2)$ satellite line of the $A^2\Sigma^+(\nu' = 0) \leftarrow X^2\Pi(\nu'' = 0)$ band. The LIF resulted from rotational transitions in the $A^2\Sigma^+(\nu' = 0) \rightarrow X^2\Pi(\nu'' = 2)$ band near 247 nm.

Mixtures were prepared by evacuating the cell to a pressure less than 2 mTorr and filling with NO to a pressure of 30 ± 5 mTorr (the uncertainty in pressure resulted mainly from outgassing and wall-adsorption effects), and filling with buffer gases to the desired total pressure ($15-100 \pm 0.1$ Torr). We measured DFWM, LIF, and absorption spectra in each mixture using two different pump-beam intensities. Line-center DFWM intensities were obtained by fitting the data with the moving-absorber line-shape expression [9] and taking the peak value of the fitted curve. To correct for the small variations in NO pressure among the mixtures we normalized the DFWM intensities by $A^2/(1-A/2)^4$, where A is the absorptivity. The numerator accounts for number density variations and the denominator accounts for beam absorption.

To obtain an experimental measure of the saturation intensity, we recorded the DFWM signal strength as a function of laser pulse energy on a pulse-by-pulse basis, as shown in Fig. 1. To determine I_{sat} we fitted the data to the equation for the saturation dependence of the stationary-absorber model [9]:

$$I_{sig} \propto \frac{I^3/I_{sat}^2}{(1+4I/I_{sat})^3}. \tag{6}$$

The effective I_{sat} obtained in this way accounts for non-uniformities in the laser beam profile, and for the real multi-level structure of the NO molecule. The best-fit I_{sat}

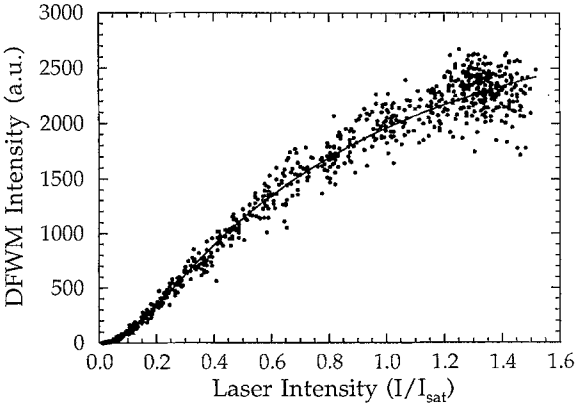

Fig. 1. Single-pulse DFWM intensity measurements of 30 mTorr of NO in 100 Torr of N_2 plotted against laser intensity. The smooth curve through the data is a fit to (6), which yields I_{sat}. These 1000 data points were aquired in 100 s

values were consistently within a factor of two of the theoretical saturation intensity calculated using the one-photon transition dipole moment μ_{12} [14], the γ_{12} and Γ_0 values discussed below, and the relation [9]

$$I_{\text{sat}} = \tfrac{1}{2}\varepsilon_0 c\hbar^2 \gamma_{12}\Gamma_0/|\mu_{12}|^2 . \tag{7}$$

For example, we obtained $I_{\text{sat}} = 0.77 \pm 0.3\,\text{MW/cm}^2$ for NO in 100 Torr of N_2, while the theoretical value was $0.58 \pm 0.1\,\text{MW/cm}^2$. In view of the simplicity of the theory and the experimental uncertainty in inferring laser intensity from measured pulse energy and estimated beam area, we consider this agreement to be excellent.

As seen in (1), DFWM intensities are strongly dependent on γ_{12}. To isolate the effect of varying Γ_0 via the changing quench rate, we chose relative pressures of N_2 and CO_2 that resulted in $\gamma_{12} = 0.0386\,\text{cm}^{-1}$ for all mixtures. (Even though quenching contributes to γ_{12}, the latter is dominated at room temperature by contributions from pure dephasing and RET processes). We computed γ_{12} from the relation

$$\gamma_{12} = p_{N_2}\gamma_{12}(N_2) + p_{CO_2}\gamma_{12}(CO_2), \tag{8}$$

where p_i and $\gamma_{12}(i)$ refer to the partial pressure and broadening coefficient for species i, respectively, $\gamma_{12}(CO_2) = 0.303 \pm 0.01\,\text{cm}^{-1}/\text{atm}$, and $\gamma_{12}(N_2) = 0.293 \pm 0.02\,\text{cm}^{-1}/\text{atm}$. Broadening coefficients were obtained from high-resolution absorption and LIF line-shape measurements, analyzed using Voigt profiles. (The second value is in excellent agreement with the coefficient reported by Chang et al. for N_2 broadening of the S_{21}-branch, with no reported N dependence [15].) Due to the similarity of the two broadening coefficients, the *total* pressures of the mixtures were varied by less than 4% in order to keep γ_{12} constant.

3 Results and Analysis

Shown in Fig. 2 are the results of DFWM intensity measurements (filled symbols) for various mixtures and for two different pump-beam intensities, corresponding to $I/I_{\text{sat}} = 0.02$ (upper panel) and $I/I_{\text{sat}} = 0.5$ (lower panel). Both saturation values are quoted for the 1:1 mixture, since I_{sat} increases by approximately 50% from left to right in the figure. The measurements at the left-most side of the plot correspond to 100 Torr of pure N_2 while those at the right-most side correspond to 96.6 Torr of pure CO_2. For both values of I/I_{sat} the signal intensity is observed to fall with increasing CO_2 mole fraction, i.e., with increasing quenching. However, the signal decrease is significantly smaller for the more strongly saturated case, approximately 15% compared to 50%. This result confirms previous indications that strongly saturated DFWM intensities are relatively insensitive to quench rate [7].

By considering the role of saturation in determining grating amplitude, we can arrive at an intuitive explanation of the effect observed in Fig. 2. According the grating description of DFWM, the probe beam and one of the pump beams interfere in the medium to form an intensity grating. If the laser is tuned to an allowed transition, an excited-state population grating is "written" in the medium, corresponding to a finite saturation of the absorption in

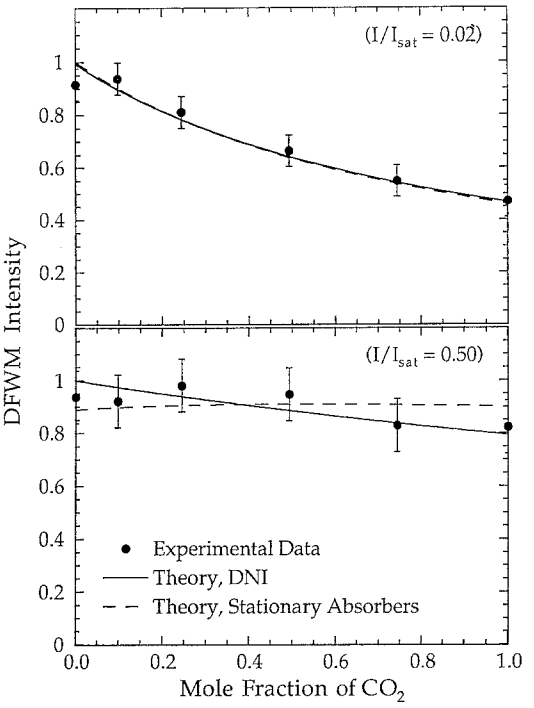

Fig. 2. Experimental and theoretical DFWM intensities of NO plotted against mole fraction of CO_2 in an N_2/CO_2 mixture, for a fixed laser intensity. The NO quench rate increases by a factor of 10^4 from left to right, while the collisional broadening γ_{12} is held constant. DNI refers to direct numerical integration of the velocity-dependent density matrix equations

the grating fringes. The other pump beam diffracts from this saturation grating, generating the signal. As the degree of saturation (ratio of I/I_{sat}) increases from a low value, the amplitude of the grating initially grows, improving its diffraction efficiency. This explains the increase of the nearly unsaturated intensities with decreasing quenching (from right to left in the upper panel of Fig. 2). However, with strong saturation the grating contrast (peak-to-valley difference in excited-state population) is nearly bleached out, so that increasing I/I_{sat} acts to increase the grating contrast and generate greater signal intensity. This tendency opposes the previous one, so we expect that for some strong saturation condition (I/I_{sat} of order 1) that the signal will be insensitive to small changes in I_{sat}, as in the lower panel of Fig. 2. It should be noted that this insensitivity also holds for other collisional processes affecting the signal via I_{sat}, including RET, VET, and elastic dephasing, as illustrated in recent DFWM intensity measurements versus buffer gas pressure [13].

To compare the experimental results of Fig. 2 with theory, it is necessary to compute Γ_0 as a function of mixture composition, which requires the RET and quench rates of NO in CO_2 and in N_2. State-to-state RET rates for the A state of NO in N_2 have been measured by Ebata et al. [16]. Based on the removal rate reported for $N = 11$ and an observed weak dependence on N, we took $\gamma_{\text{RET2}}(N_2) = 1.06 \times 10^{10}\,\text{s}^{-1}\,\text{atm}^{-1}$. The weak N-dependence is consistent with X-state linewidths measured by infrared spectroscopy for NO perturbed by N_2 [17]. Moreover, the infrared linewidths yield upper bounds for the X-state removal rates that compare well with removal rates measured

in pump/probe experiments by Sudbø and Loy [18]. Both sets of X-state rates agree within experimental uncertainties with the A-state rates of Ebata et al., leading us to assume $\gamma_{RET1} = \gamma_{RET2}$. Unfortunately, there appear to be no reliable RET measurements for NO perturbed by CO_2. Broida et al. [12] report RET rates for NO colliding with CO_2 and N_2, but their N_2 rates are approximately a factor of four lower than those of [16–18]. Assuming that an error in absolute magnitude caused the discrepancy, we used a ratio of the Broida et al. RET rates for CO_2 relative to N_2 to scale the N_2 rate of Ebata et al. This resulted in a CO_2 rate that was 28% larger than the corresponding N_2 rate, and a factor of two larger than gas kinetic [19]. Extensive measurements of the NO A-state quenching cross-sections by CO_2 and N_2 have been recently reported [8]. At room temperature N_2 is found to be an extremely inefficient quencher ($\gamma_{Quench}(N_2) = 1.14 \times 10^6\ s^{-1}\ atm^{-1}$) compared to CO_2 ($\gamma_{Quench}(CO_2) = 9.1 \times 10^9\ s^{-1}\ atm^{-1}$). Using these results together with the above RET rates, using (2), (4), and (5), and computing the net γ_{Quench} similarly to (8), we find that Γ_0 (half width at half maximum) varies from $0.0075\ cm^{-1}$ in the NO–N_2 mixture to $0.0116\ cm^{-1}$ in the NO–CO_2 mixture. Thus, the effect on Γ_0 by the enormous change in quench rate across these mixtures is largely masked by RET.

Similarly, the effect on γ_{12} by the large change in quench rate is largely masked by pure dephasing. From (2), we see that up to 80% of γ_{12} results from elastic dephasing collisions (recall that in this experiment, γ_{12} is constant and equal to $0.0386\ cm^{-1}$, corresponding to $7.27 \times 10^9\ s^{-1}$). Since we have intentionally kept γ_{12} constant in this experiment, the effects of quenching on the total dephasing rate are not investigated here.

The dashed lines in Fig. 2 indicate predictions of the stationary-absorber theory based on experimental values of I/I_{sat} and the previously discussed values of Γ_0. A best-fit scaling factor has been applied for comparison with the data. In the limit of weak saturation the theoretical signal varies according to $1/\Gamma_0^2$ [see (1)], and therefore decreases moderately with quenching, in good agreement with experiment. For the saturated case, the theory is essentially flat and does not capture the downward trend of the data with increasing quenching. The solid lines in Fig. 2 are the results of the DNI calculations. In the upper panel, the DNI curve is nearly identical to the stationary-absorber theory since both models approach (1) in the limit of low saturation. However, the saturated measurements are better described by the DNI calculation, which indicates a slight downward trend with increasing quenching. This improved agreement is likely the result of accounting for the use of pulsed lasers and including the inhomogeneous broadening of the NO absorbers ($0.1\ cm^{-1}$ FWHM).

Compared to DFWM, simultaneously measured LIF intensities were observed to vary much more dramatically with quench rate. The symbols in Fig. 3 indicate unsaturated DFWM and LIF measurements for several mixtures of CO_2 and N_2. The experimental conditions are identical to those previously discussed, with γ_{12} held constant. Note that the DFWM measurements appear nearly constant on this log plot, while the LIF measurements are severely attenuated as quenching increases from left to right. In fact, the LIF intensity is attenuated by a factor of 370, while the DFWM intensity decreases by a factor of 2. DFWM is clearly less sensitive to quench rate than LIF under these conditions.

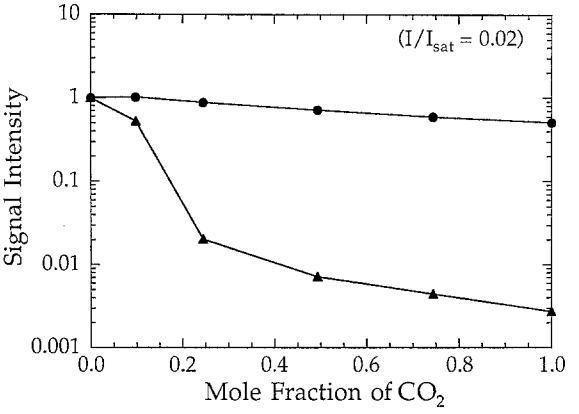

Fig. 3. Nearly unsaturated experimental DFWM (*circles*) and LIF (*triangles*) signal intensities versus mole fraction of CO_2 in an N_2/CO_2 mixture. The data are normalized to 1.0 at the left axis and are connected by straight lines to guide the eye

Figure 4 shows a theoretical comparison of the sensitivity of both LIF and DFWM to quenching in typical combustion environments. For simplicity, the stationary-absorber model [9] was chosen to analyze DFWM's sensitivity to quenching. Likewise, a simple two-level model including saturation [1] was used to illustrate the sensitivity of LIF. In this study, sensitivity is defined as:

$$\text{Sensitivity} \equiv \frac{\partial I_{sig}}{\partial \gamma_{Quench}}\bigg|_{\gamma_{Quench}} \Big/ \frac{I_{sig}}{\gamma_{Quench}} \approx \frac{\Delta I_{sig}}{I_{sig}} \Big/ \frac{\Delta \gamma_{Quench}}{\gamma_{Quench}}. \quad (9)$$

where I_{sig} is the LIF or DFWM signal intensity. Thus, the sensitivity is the fractional change in signal intensity per fractional change in quench rate. The parameters chosen for study are typical for an atmospheric pressure, methane-

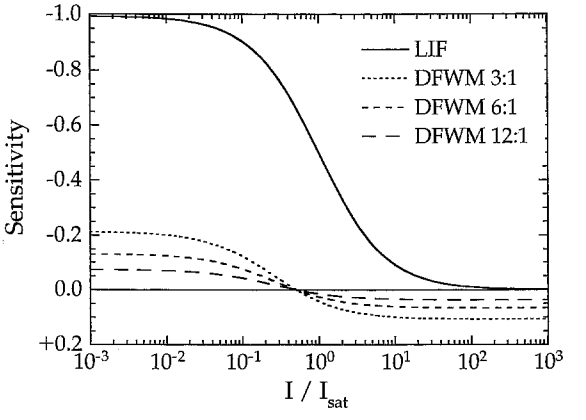

Fig. 4. Sensitivity of DFWM and LIF to quenching. The LIF curve was calculated assuming the ratio $\gamma_{Quench}:\gamma_{Natural} = 1:1/150$. DFWM curves were calculated assuming the ratios of $\gamma_{RET}:\gamma_{Quench} = 3:1$, 6:1, and 12:1, as indicated. The conditions roughly correspond to the maximum quench rate in a methane-air diffusion flame at 2150 K, which obeys $\gamma_{RET}:\gamma_{Quench}:\gamma_{Natural} = 6:1:1/150$

air diffusion flame. We estimated that for NO, the ratio $\gamma_{RET}:\gamma_{Quench}:\gamma_{Natural}$ is approximately 6:1:1/150 in regions of maximum quenching [8, 17, 20]. As shown in the figure, for $I/I_{sat} \ll 1$, a 1.0% increase in quenching causes nearly the same decrease in LIF intensity, while for DFWM the same change in quenching results only in a 0.13% decrease in intensity. DFWM curves calculated using $\gamma_{RET}:\gamma_{Quench}$ equal to 3:1 and 12:1, respectively, are also shown to illustrate the sensitivity of the signal intensity to RET variations.

As the laser intensity increases, the signal intensities of both techniques become less sensitive to quenching as shown in Fig. 4. According to the stationary absorber model, the DFWM signal achieves complete independence of quenching at $I/I_{sat} = 0.50$. DNI calculations, which include the Doppler effect and the effects of the finite laser pulse length, predict a similar independence of quenching at $I/I_{sat} \approx 1.0$ [10]. Note that LIF requires $I/I_{sat} \gg 1$ for the signal to become independent of quenching. It is even more difficult to reach complete saturation using LIF because of the relative contribution to the fluorescence from the low-intensity wings of the spatial profile of the laser beam. This contribution increases compared to the contribution from the center of the spatial profile as the laser intensity increases [21]. For similar reasons, it is necessary also to resolve the saturated LIF signal temporally and to measure the signal at the peak of the laser pulse [22]. It is especially difficult to reach the fully saturated limit for the case of two-dimensional imaging in atmospheric pressure flames. The fact that DFWM signals are nearly independent of collision rates at $I/I_{sat} \approx 1$ is a great advantage because the bulk of the signal still comes from the center of the laser beam spatial and temporal profiles at these intensities. Thus, so-called "wing" effects should be much less important for saturated DFWM measurements than for saturated LIF measurements.

The fact that the effects of collisional transfer rates on the DFWM signal is minimized for $I/I_{sat} \approx 1$ is advantageous for several other reasons. Assuming that the main source of noise is due to scattered light from the probe beam, Williams et al. have shown that the optimum signal-to-noise ratio occurs for $I/I_{sat} \approx 1$ [23]. Lucht et al. have shown that the effects of the total dephasing rate, γ_{12}, in (1) and (2), are minimized near $I/I_{sat} \approx 1$ [10]. Finally, at $I/I_{sat} \approx 1$ and higher intensities, the DFWM signal has a reduced dependence on laser intensity, reducing the effects of shot-to-shot fluctuations and laser-sheet profile variations for point and/or imaging measurements [14].

Collisional quenching can also result in a second important effect in DFWM not described above. Quenching of the molecules excited in a population grating can lead to spatially modulated deposition of heat, forming a "thermal grating". The resulting temperature, pressure and density perturbations cause a refractive index modulation that can diffract the pump beams and generate a DFWM signal. In some circumstances, these thermal gratings can have very large diffraction efficiencies which dominate those of population gratings. We are currently investigating these effects in more detail [24]. For the gas pressures used in this experiment, the effects of thermal gratings were found to be negligible.

4 Conclusions

In conclusion, DFWM intensities have been shown to be significantly less sensitive to quench-rate variations than LIF, under conditions where homogeneous broadening is insensitive to quench rate. Such conditions are encountered to a great extent in flames, where homogeneous broadening is usually dominated by rotational relaxation [1] or pure dephasing, and occasionally by predissociation [25]. For small molecules of combustion interest, quenching usually proceeds more slowly than gas-kinetic collision rates, while rotational transfer rates are typically comparable to gas kinetic rates [26]. The effects of quenching variations will thus be largely masked by rotational relaxation. Rotational relaxation rates can still vary with collision partner, but such variations will generally be less severe than those of quench rates. For example, at flame temperatures Thoman et al. [8] have measured NO quench rates that vary by nearly two orders of magnitude for species such as N_2 and H_2O, while NO rotational transfer rates vary by less than a factor of two for a variety of perturbers [13].

Intensity measurements performed with $I/I_{sat} \ll 1$ are in excellent agreement with a steady-state, two-level theory for stationary absorbers and with numerical solutions of the time-dependent density matrix equations for moving absorbers. Measurements obtained with saturating intensities are better described by the time-dependent calculations, as a result of including absorber motion and transient effects of the 10 ns laser pulse. Furthermore, the calculations showed that sensitivity to quenching is minimized for $I/I_{sat} \approx 1$, an intensity which additionally optimizes other properties of DFWM.

Acknowledgements. This work was supported by the U.S. Department of Energy, Office of Basic Energy Sciences, Division of Chemical Sciences and the Office of Industrial Technologies, Division of Advanced Industrial Concepts. Partial support for PMD was provided by the Air Force Office of Scientific Research, Aerospace Sciences Directorate, and for RLF by the California Institute for Energy Efficiency.

References

1. A good review of LIF and other combustion diagnostics is found in A.C. Eckbreth: *Laser Diagnostics for Combustion Temperature and Species* (Abacus, Cambridge, MA 1988)
2. D.J. Rakestraw, R.L. Farrow, T. Dreier: Opt. Lett. **15**, 709–711 (1990)
3. P. Ewart, M. Kaczmarek: Appl. Opt. **30**, 3996–3999 (1991)
4. B. Yip, P.M. Danehy, R.K. Hanson: Opt. Lett. **17**, 751–753 (1992)
5. I.P. Jefferies, A.J. Yates, P. Ewart: *Coherent Raman Spectroscopy Application and New Developments*, ed. by E. Castellucci (World Scientific, Singapore 1992)
6. D.S. Green, T.G. Owano, S. Williams, D.G. Goodwin, R.N. Zare, C.H. Kruger: Science **259**, 1726–1729 (1993)
7. T. Dreier, D.J. Rakestraw: Opt. Lett. **15**, 72–74 (1990)
8. J.W. Thoman, Jr., J.A. Gray, J.L. Durant, Jr., P.H. Paul: J. Chem. Phys. **97**, 8156–8163 (1993)
   J.A. Gray, P.H. Paul, J.L. Durant: Chem. Lett. **190**, 266–270 (1992)
9. R.L. Abrams, J.F. Lam, R.C. Lind, D.G. Steel, P.F. Liao: Phase conjugation and high-resolution spectroscopy by resonant degenerate four-wave mixing. In *Optical Phase Conjugation* ed. by R.A. Fisher (Academic, New York 1983) pp. 211–284
10. R.P. Lucht, R.L. Farrow, D.J. Rakestraw: J. Opt. Soc. Am. B **10**, 1908–1920 (1993)

11. S. Stenholm: *Foundations of Laser Spectroscopy* (Wiley, New York 1984) pp. 35, 74
12. H.P. Broida, T. Carrington: J. Chem. Phys. **38**, 136–147 (1963)
13. R.L. Farrow, D.J. Rakestraw: Science **257**, 1894–1900 (1992)
14. R.L. Farrow, D.J. Rakestraw, T. Dreier: J. Opt. Soc. Am. B **9**, 1770–1777 (1992). In calculating $|\mu_{12}|^2$ these authors mistakenly adjusted the $O_{12}(2)$ line strength cited in Ref. [20] of their paper. Using the correct line-strength value of 1.94, $|\mu_{12}|^2$ is computed to be 2.7×10^{-62} C^2m^2
15. A.Y. Chang, M.D. DiRosa, R.K. Hanson: J. Quant. Spectrosc. Radiat. Transfer **47**, 375–390 (1992)
16. T. Ebata, Y. Anezaki, M. Fujii, N. Mikami, M. Ito: Chem. Phys. **84**, 151–157 (1984)
17. P.K. Falcone, R.K. Hanson, C.H. Kruger: J. Quant. Spectrosc. Radiat. Transfer **29**, 205–221 (1983)
18. A.S. Sudbø, M.M.T. Loy: J. Chem. Phys. **76**, 3646–3654 (1982)
19. J.T. Yardley: *Introduction to Molecular Energy Transfer* (Academic, New York 1980) pp. 15–20
20. P.H. Paul, J.A. Gray, J.L. Durant, Jr., J.W. Thoman, Jr.: AIAA Journal (submitted)
21. J. Daily: Appl. Opt. **17**, 225–229 (1978)
22. R.P. Lucht, D.W. Sweeney, N.M. Laurendeau: Combust. Flame **50**, 189–205 (1983)
23. S. Williams, D.S. Green, S. Sethuraman, R.N. Zare: J. Am. Chem. Soc. **114**, 9122–9130 (1992)
24. P.M. Danehy, E.J. Friedman-Hill, P.H. Paul, R.L. Farrow: J. Opt. Soc. Am. B., to be submitted
25. R.A. Copeland, J.B. Jeffries, D.R. Crosley: J. Mol. Spectrosc. **143**, 183–185 (1990)
26. J.H. Bechtel, C.J. Dasch, R.E. Teets: Combustion research with lasers, *Laser Applications*, ed. by J.F. Ready, R.K. Erf (Academic, New York 1984) p. 145